Zero-field splitting of the $4f^7$ state: An electrostatic theory for Gd^{3+}-M^+ complexes in CaF_2

E. J. Bijvank and H. W. den Hartog
Solid State Physics Laboratory, 1 Melkweg, 9718 EP Groningen, The Netherlands
(Received 10 April 1980)

From the known bulk properties of CaF_2 crystals and the theoretical parameters of the impurity ions Gd^{3+} and M^+ (M = Li, Na, ... Cs) describing the Coulomb, polarization, and the repulsive interactions with neighboring ions in the crystal lattice, we have calculated the ionic positions associated with minimum total potential energy as a function of the M^+ radius. These results have been employed to evaluate the behavior of the crystal-field parameters c_1^0, B_2^0, and B_2^2, which has been investigated extensively with various experimental techniques in earlier papers from this laboratory. It is concluded from the results given in this paper that with the electrostatic model employed here the crystal-field parameters mentioned above can be described quite well. For the parameter B_2^2 it is suggested that it is necessary to allow rather large numbers of ions neighboring the Gd^{3+}-M^+ complex to relax towards new equilibrium positions.

I. INTRODUCTION

Because we want to assess the capabilities of the point-charge model in calculating the magnetic crystal-field parameters B_2^0 and B_2^2 for Gd^{3+} impurities in ionic materials, it is of importance to determine the ionic positions in the immediate surroundings of the Gd^{3+}-M^+ complex independently. In this paper we present a calculation based upon the polarizable-point-charge model to evaluate the minimum potential energy with respect to the ionic positions. These defect-modeling calculations have been applied in the literature to treat many different types of defects.[1,2]

Besides the polarizable-point-charge model, various shell models have been used in the literature.[3,4] From diffraction experiments it is concluded that in CaF_2 the ions are well-defined entities[5]; also it has been shown that CaF_2 is an ideal ionic material.[6] We expect to obtain reliable results employing the polarizable-point-charge model because in our approach we focus our attention on the trends of the magnetic parameters as a function of the ionic radius of the monovalent-cation impurity. It is rewarding, that also the absolute values of B_2^0 and c_1^0 calculated are in good agreement with experiment.

II. DESCRIPTION OF THE CALCULATION

The calculations carried out in this paper are based upon the polarizable-point-ion (PPI) model, implying that in the CaF_2 lattice the host Ca and F ions are represented by charges $+2e$ and $-e$, respectively. The electronic polarizabilities of the Ca^{2+} and F^- ions are chosen to be $\alpha(Ca^{2+}) = 0.98$ Å^3 and $\alpha(F^-) = 0.76$ Å^3 in accordance with Franklin.[1] The repulsive interactions are described in terms of Born potentials which have been modified such that for two ions with an interionic distance smaller than 85% of the sum of their ionic radii, the repulsive energy becomes very large (hard cores). The van der Waals interactions are included implicitly in the repulsion terms because of the relatively low electronic polarizabilities of the host lattice ions.

When impurity ions are introduced into the CaF_2 lattice the total energy of the new system contains contributions from (i) the effective charges of the impurities, (ii) the changes of the repulsive interactions, (iii) polarization effects, and (iv) effects associated with relaxations of the ions of the surrounding lattice.

In the systems under investigation (Gd^{3+}-M^+ in CaF_2) we are dealing with two effective charges which polarize the surrounding lattice. We emphasize that the effects of the induced dipoles are appreciable here, in contrast with the results of van Winsum *et al.*[7,8] for $SrCl_2$:Mn^{2+} and KCl:Li^+ where the valency of the impurities are equal to the valency of the ions which have been substituted. In this work we have applied a defect modeling computer program that evaluates the minimum total energy of a crystal with respect to variations of the positions of a collection of ions in the neighborhood of the impurity ions. In order to demonstrate the limitations of the model due to too small a number of relaxing ions we shall present some results (A) obtained for a system containing 24 of these ions; the corresponding region is referred to as region I. More accurate results (B) are obtained when we extend region I to 44 ions. The charges and induced dipoles present in region I are allowed to interact electrostatically; also repulsive interactions between nearest neighbors and next-nearest neighbors are taken into account.

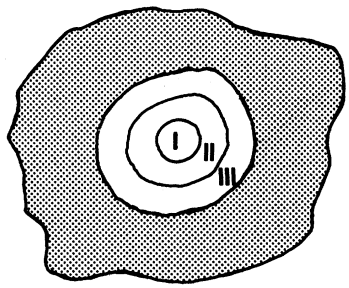

FIG. 1. In the calculation of the total energy the crystal is divided into a number of regions; the complex is situated in region I.

In addition we define a second and third collection of surrounding ions which are not allowed to relax, but the ions in these regions can be polarized. In region II the ions are polarized by the charges and induced dipoles present in region I and by the induced dipoles present in regions II and III. This implies that the induced dipoles must be calculated self-consistently; in our program we employ an iteration method as described by Bijvank and den Hartog in the preceding paper.[9] For ions more distant than those in region II we assume that the induced dipoles are due to charges in region I. For the calculations of type *A* (less accurate method) region II contains 70 and region III 180 ions (see Fig. 1). The calculations *B* are carrried out with 246 ions in region II; the effect of polarization of more distant ions (region III) has been neglected. Finally, we note that in accordance with van Winsum *et al.*[7] we have taken into account the contributions due to point charges present at unperturbed lattice sites; these contributions have been expanded in a Taylor series. This series clearly also consists of contributions from point charges at the unperturbed lattice positions of region I; therefore we have corrected the above-mentioned contributions of region I as explained below.

An important reason for Catlow and Norgett[10] not to use the polarizable-point-charge model but one of the shell models is the occurrence of a "polarization catastrophe." It is easy to show from the treatment given by Böttcher[11] that a polarization catastrophe does not occur at interionic distances larger than about $\frac{1}{2}(r_1+r_2)$ where r_1 and r_2 are the radii of the ions under consideration. From this it follows that possible polarization catastrophes are caused by deficiencies of the model used. It our calculations we have not observed these polarization catastrophes whenever the iterative process to account for dipole-dipole interactions is included in the minimization.

The total energy of the crystal consists of three main contributions:

(i) Coulomb interactions: we define a deviation ΔE_s from the perfect lattice energy, which can be written as

$$\Delta E_s = \sum_{\substack{j>i \\ j,i\in C}} \left(\frac{e_i' e_j'}{|\vec{r}_i' - \vec{r}_j'|} - \frac{e_i e_j}{|\vec{r}_i - \vec{r}_j|} \right) , \tag{1}$$

where $i \in C$ means that we sum over an appreciable part of the crystal ($\sim 10^6$ ions) considered.

(ii) Polarization interactions: ΔE_p is the variation of the total energy due to the interaction between point charges and induced dipoles and the interaction between induced dipoles; the self-energy of the system of induced dipoles is also included

$$\Delta E_p = -\frac{1}{2} \sum_{i\in C} \alpha_i' (\vec{E}^{(i)\prime}_{\text{point charges}} + \vec{E}^{(i)\prime}_{\text{induced dipoles}}) \times \vec{E}^{(i)\prime}_{\text{point charges}} , \tag{2}$$

for the two particle problem this formula has been derived by Böttcher.[11]

(iii) Repulsive energy: The variation of the repulsive interaction due to the presence of the impurities can be written as

$$\Delta E_r = \sum_{\substack{j>i \\ j,i\in C}} [\phi_{ij}'(\vec{r}_i' - \vec{r}_j') - \phi_{ij}(\vec{r}_i - \vec{r}_j)] . \tag{3}$$

In Eqs. (1), (2), and (3) the primes refer to the actual charges, polarizabilities, positions, and repulsive potentials in the crystal. The unprimed quantities in the energy expressions are associated with the pure CaF_2 lattice.

In order to calculate the energy efficiently it is necessary to separate the contributions connected with the regions I, II, and III and because we want to employ the Taylor-series expansion given by van Winsum *et al.*[7] we have to rewrite Eq. (1) as follows

$$\Delta E_s = \sum_{i\in \mathrm{I}} \left(\sum_{\substack{j\in \mathrm{I} \\ j>i}} \frac{e_i' e_j'}{|\vec{r}_i' - \vec{r}_j'|} - \sum_{\substack{j\in \mathrm{I} \\ j\neq i}} \frac{e_i' e_j'}{|\vec{r}_i' - \vec{r}_j'|} \right) + \sum_{i\in \mathrm{I}} e_i' V(\vec{r}_i' - \vec{r}_i) + \sum_{\substack{i\in \mathrm{I} \\ i\neq \mathrm{Gd}}} \frac{e_i'}{|\vec{r}_i' - \vec{r}_{\mathrm{Gd}}|} - \sum_{\substack{i\in \mathrm{I} \\ i\neq M}} \frac{e_i'}{|\vec{r}_i' - \vec{r}_M|}$$

$$+ \sum_{i\in \mathrm{I}} \sum_{j\in R} \left(\frac{e_i' e_j}{|\vec{r}_i - \vec{r}_j|} - \frac{e_i e_j}{|\vec{r}_i - \vec{r}_j|} \right) + \sum_{\substack{i\in \mathrm{I} \\ i\neq j}} \sum_{j\in \mathrm{I}} \frac{e_i' e_j}{|\vec{r}_i - \vec{r}_j|} - \sum_{\substack{i\in \mathrm{I} \\ j>i}} \sum_{j\in \mathrm{I}} \frac{e_i e_j}{|\vec{r}_i - \vec{r}_j|} . \tag{4}$$

TABLE I. A summary of the polarizabilities and the repulsive parameters, used as input parameters in the computer calculations. The parameters deduced from the physical properties of pure CaF_2 are taken from Franklin (Ref. 1). The parameters concerning the impurities Gd^{3+} and M^+ have been collected from Catlow *et al.* (Ref. 12) and Boswarva and Lidiard (Ref. 13).

	Lattice constant: 5.436 Å		
Ion	Polarizability (Å^3)	Ion	Polarizability (Å^3)
F^-	0.76	Na^+	0.255
Ca^{2+}	0.98	K^+	1.201
Gd^{3+}	1.04	Rb^+	1.797
Li^+	0.029	Cs^+	3.137
ion i-ion j	B_{ij} (10^{-10} erg)	ρ (Å)	
F^--F^-	7.33	0.282	
Ca^{2+}-F^-	27.46	0.282	
Ca^{2+}-Ca^{2+}	102.96	0.282	
Gd^{3+}-F^-	60.00	0.282	
Li^+-F^-	2.40	0.291	
Na^+-F^-	6.41	0.296	
K^+-F^-	12.44	0.315	
Rb^+-F^-	15.10	0.323	
Cs^+-F^-	28.06	0.323	

Here $i \in \mathrm{I}$ means that the summation is carried out over the ions in region I and $j \in R$ refers to contributions from all ions outside region I but inside C. The last three terms in Eq. (4) are omitted in our computer calculations since they do not depend on the actual positions of the ions in region I.

The electric fields occurring in Eq. (2) are calculated as described in the preceding paper[9] (Appendix A). We note that in the present paper the formulas have been given in cgs units, whereas in the preceding paper we have worked the SI units. The repulsive potentials used in the calculations are of the Born type and can be written as

$$\phi_{ij}(\vec{r}_i - \vec{r}_j) = B_{ij} \exp(-|\vec{r}_i - \vec{r}_j|/\rho_{ij}) \quad . \tag{5}$$

A compilation of the important parameters used in the calculations has been given in Table I.

It is obvious that the number of relaxing ions (region I) is limited by the computation times necessary to minimize the total energy of the crystal containing the two impurities Gd^{3+} and M^+. In addition the computation of the self-consistent electric fields felt by the ions in regions I and II is rather time consuming. It is possible to make the corresponding iteration process highly efficient by calculating the electric fields in an order of succession such that in the beginning the corrections for $\vec{E}$ are small; also it is found useful to employ the calculated electric field strengths and dipoles immediately in the evaluations of the next $\vec{E}$ corrections. As the system approaches the minimum conditions the corrections for the electric fields added to the previously calculated ones are reduced dramatically; therefore it was found not necessary to iterate more than once for each energy evaluation. By suitably combining the minimization and iteration processes it was possible to reduce the computation times significantly, allowing us to extend regions I and II to sizes corresponding with the calculations of type B; these methods have been developed by Hess.[14]

The minimization of the total energy of the system provides us with the equilibrium positions of all ions in region I. Using these positions and those in the remainder of the crystal we can calculate the electrostatic crystal-field potential at the Gd^{3+} ion, which is expanded in a series of homogeneous polynomials

$$V(\vec{r}) = c_0^0 + c_1^0 P_1^0 + c_2^0 P_2^0 + c_2^2 P_2^2 + c_3^0 P_3^0 + c_3^2 P_3^2 + c_4^0 P_4^0 + \cdots \quad , \tag{6}$$

where P_l^m are defined by Abragam and Bleaney.[15] The expressions for c_l^m have been given in Appendix A of the preceding paper and contain contributions from point charges and induced dipoles. The method used to calculate the induced dipoles has also been described in Appendix A of the preceding paper.

Although our EPR results allow us to calculate the crystal-field parameters B_l^m of the spin Hamiltonian [see Bijvank *et al.*,[16] Eq. (1)] for $l = 4$ and 6 we cannot use this information to test the electrostatic potential because the connection between the magnetic parameters B_l^m and the electrostatic ones c_l^m is highly uncertain for $l > 2$. Therefore we restrict ourselves to testing the parameters c_1^0, c_2^0, and c_2^2. An outline

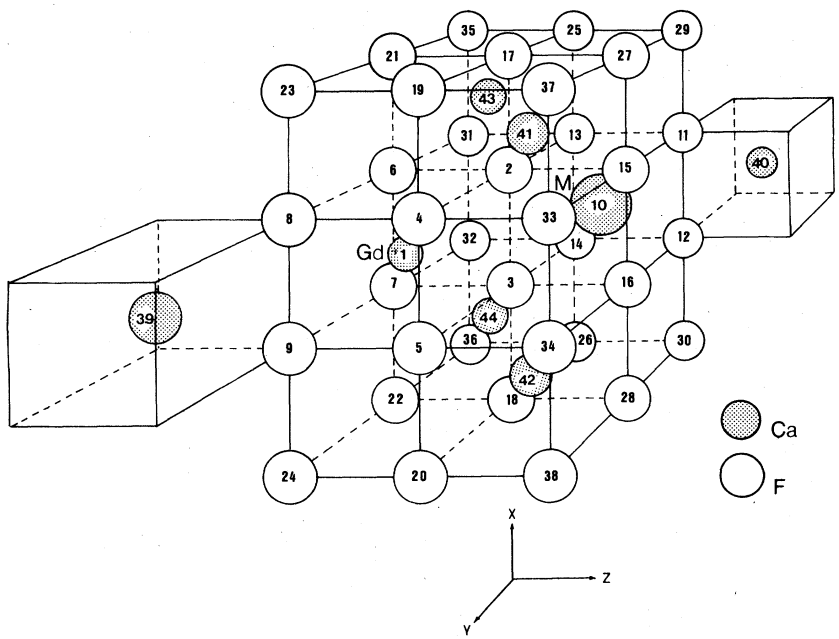

FIG. 2. Schematic three-dimensional representation of region I. In the calculations of type A region I contains the first 24 ions indicated in this figure; in the calculations of type B region I contains 44 ions. Ion 1 represents the Gd^{3+} ion, ion 10 the M^+ ion.

of the method used for the calculation of the parameters B_l^m from c_1^0, c_2^0, and c_2^2 has been presented by Lefferts *et al.*[17]

III. RESULTS OF THE CALCULATIONS

A. Calculations of type A

In order to find a measure for the quality of the calculations, we have checked the unperturbed cubic CaF_2 lattice using the parameters of Table I. The calculations were started with ionic positions in region I which differed from lattice sites. We found that after minimization of the energy the displacement parameters were equal to zero with 5×10^{-4} Å. Region I contains 24 ions and is shown schematically in Fig. 2.

The introduction of trivalent Gd in the CaF_2 lattice is now considered in a situation of nonlocal charge compensation; i.e., the interstitial fluoride ion that is formed is assumed to be far away from the Gd impurity. If the surrounding ions forming region I are chosen such that the Gd^{3+} ion is at the center of region I, the calculated positions of the ions in region I are in accordance with cubic symmetry within reasonable error bars. If, on the other hand, region I is chosen as depicted in Fig. 2 (ions 1–24), the result is a noncubic situation; the symmetry of the displacements within region I is C_{2v}, which corresponds with the symmetry of the collection of ions within region I. The displacements of the most important ions in region I are given in Fig. 3. Associated with this situation we find $B_2^0=-39.7$ G, $B_2^2=-36.5$ G, and $c_1^0=-2.9\times10^9$ V/m. From these values compared to the experimental ones[16] we conclude that the number of ions in region I is too small to describe the physical properties of cubic Gd^{3+}. We have to limit the number of ions in regions I and II in the calculations of orthorhombic Gd^{3+}-M^+ complexes; therefore it is impossible to choose an array of lattice points surrounding the Gd^{3+} impurity which is large enough to describe cubic Gd^{3+} as well as the specific features of the M^+ impurity. The existence of the above mentioned contributions to B_2^0, B_2^2, and c_1^0, however, is not very important in our approach; we

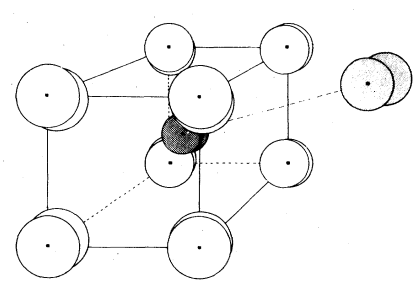

FIG. 3. Schematic three-dimensional representation of some calculated positions and lattice positions of the ions around a "cubic" Gd^{3+} ion in CaF_2. The Gd^{3+} ion lies inside the cube of the eight fluorine ions. The other cation in the figure represents a Ca^{2+} ion; the direction of the shift of this ion is away from the Gd^{3+} ion. All deviations from cubic symmetry have been enlarged by a factor of 3.

TABLE II. Calculated displacements in Å with respect to pure CaF_2 for the most important ions in region I; this calculation corresponds with method *A* in the text. The numbers in this table, which indicate the ions in region I, correspond with the numbers in Fig. 2; the system of axes has been given in Fig. 2. Displacements of ions occupying symmetrical positions with respect to the complex can be deduced from the displacements by symmetry operations.

		Li^+	Na^+	K^+	Rb^+	Cs^+
ion 1:	Δx	0	0	0	0	0
	Δy	−0.128	−0.116	−0.020	0.042	0.108
	Δz	0.128	0.116	0.020	−0.042	−0.108
ion 2:	Δx	−0.071	−0.053	0.004	0.059	0.121
	Δy	−0.104	−0.079	0.013	0.090	0.144
	Δz	0.104	0.079	−0.013	−0.090	−0.144
ion 4:	Δx	−0.024	−0.032	−0.034	−0.055	−0.071
	Δy	−0.049	−0.040	0.014	0.063	0.089
	Δz	−0.022	−0.017	−0.058	−0.085	−0.099
ion 8:	Δx	−0.029	−0.021	−0.040	−0.036	−0.039
	Δy	−0.029	−0.030	−0.003	0.015	0.026
	Δz	0.029	0.030	0.003	−0.015	−0.026
ion 10:	Δx	0	0	0	0	0
	Δy	−0.301	−0.394	−0.120	−0.058	−0.188
	Δz	0.301	0.394	0.120	0.058	0.188

mainly concentrate on the variations of these parameters as a function of the M^+ radius.

We now simulate an orthorhombic complex by introducing the charge associated with the substitutional M^+ impurities neighboring the Gd^{3+} ion, in addition the repulsive interactions associated with the impurity are different from those of the corresponding host ions. The computed displacements for ten important ions of the defect system have been compiled in Table II and a review of the results for all ions in region I has been depicted in Fig. 4. It should be noted that in Fig. 4 all deviations from the lattice

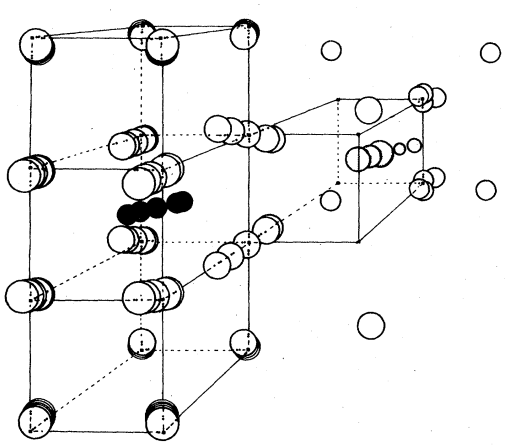

FIG. 4. Schematic three-dimensional representation of the positions of the ions in region I, resulting from calculations of type *A* (see also Table II). All 24 ions of region I have been indicated in the figure; for clarity the displacements from the lattice sites have been enlarged by a factor of 3. The Gd^{3+} ion is represented by a black sphere, the M^+ ion by a grey sphere of varying radius.

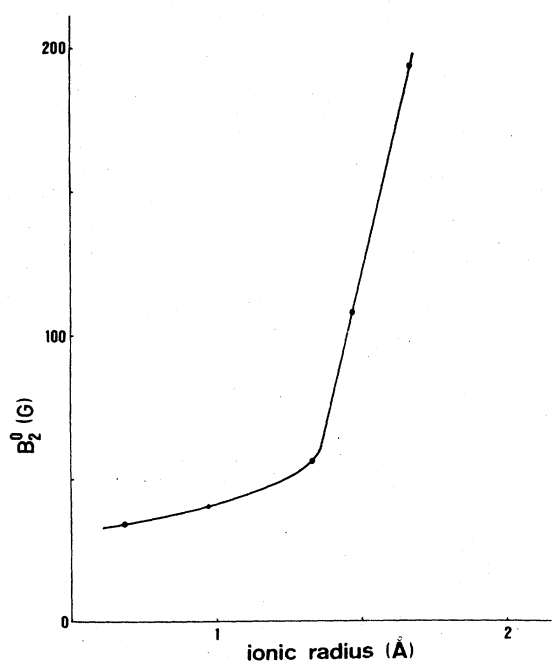

FIG. 5. Calculated values, as given in Table III, of the magnetic crystal-field parameter B_2^0 as a function of the radius of the M^+ ion.

TABLE III. Calculated and experimental values of the crystal-field parameters B_2^0, B_2^2, and c_1^0. The calculated values have been obtained from the results of method A and formulas (3) and (4) (given in the preceding paper).

	B_2^0 (calc) (G)	B_2^0 (expt) (G)	B_2^2 (calc) (G)	B_2^2 (expt) (G)
Li^+	34.5	17.7	92.6	−46.3
Na^+	41.2	3.4	85.7	−30.0
K^+	56.4	83.6	66.7	−20.1
Rb^+	108.4	141.8	62.0	−11.9
Cs^+	194.3	220.5	51.6	−4.0
	c_1^0 (calc) (10^9 V/m)	c_1^0 (expt) (10^9 V/m)		
Li^+	−4.4	±11.3		
Na^+	−4.6	±10.7		
K^+	1.4	±6.3		
Rb^+	5.0	±3.2		
Cs^+	10.3	...		

configuration have been magnified in order to give a clear review of the shifts of the ions in region I.

From the calculated positions of the ions we have calculated the magnetic parameters B_2^0 and B_2^2 and the odd crystal-field parameter c_1^0. The results have been given in Table III and Figs. 5, 6, and 7.

B. Calculations of type *B*

As mentioned before, in these calculations region I is extended to 44 ions (see Fig. 2); this implies that the number of displacement parameters in C_{2v} point-group symmetry is 37. Similar to the calculations of type A we have performed a minimization of the potential energy for a trivalent Gd ion without a charge compensating M^+ impurity in the immediate vicinity. It appears that the impurity ion is located at the lattice position, while the surrounding ions show displacements of 4×10^{-3} to 0.1 Å. The largest displacements are found for two of the nearest Ca^{2+} ions (ions 10 and 39); the relaxations of these ions are in outward directions with respect to the Gd^{3+} ion.

Starting with the calculated configuration we have evaluated the crystal-field parameters and the results obtained are $B_2^0=70.9$ G, $B_2^2=-6.1$ G, and $c_1^0=-4.8\times10^9$ V/m. This result shows that also in the present calculations the size of region I is chosen too small; the asymmetry of region I induces the crystal-field parameters of degree lower than 4. It is impossible, however, to increase the size of region I significantly because of the extremely long computing times.

We note that in the calculations of this type we have introduced a "hard core" for each of the ions in region I; for the F^- ions we have chosen R(hard core) = 1.25 Å, for Ca^{2+} R(hard core) = 0.90 Å. For

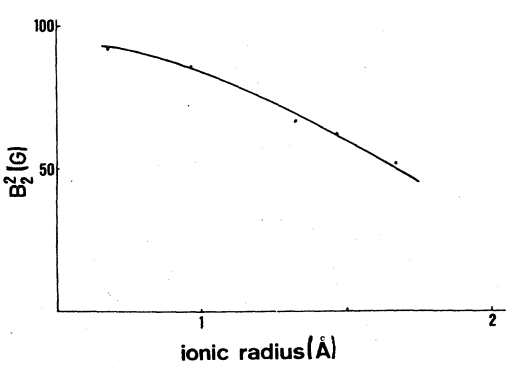

FIG. 6. Calculated values of the magnetic crystal-field parameter B_2^2, given in Table III, as a function of the radius of the M^+ ion.

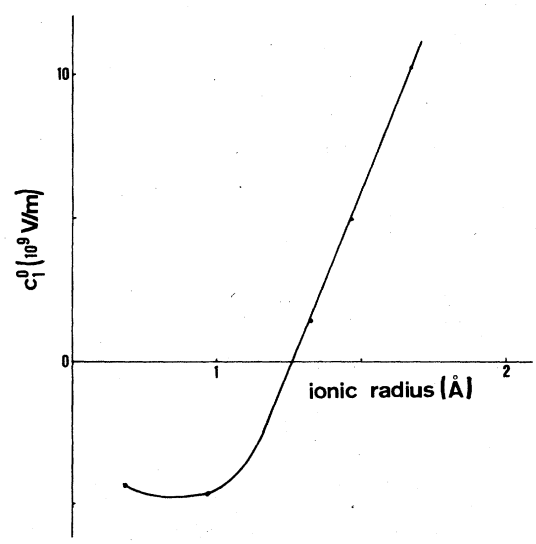

FIG. 7. Calculated values of the electrostatic crystal-field parameter c_1^0, given in Table III, as a function of the radius of the M^+ ion.

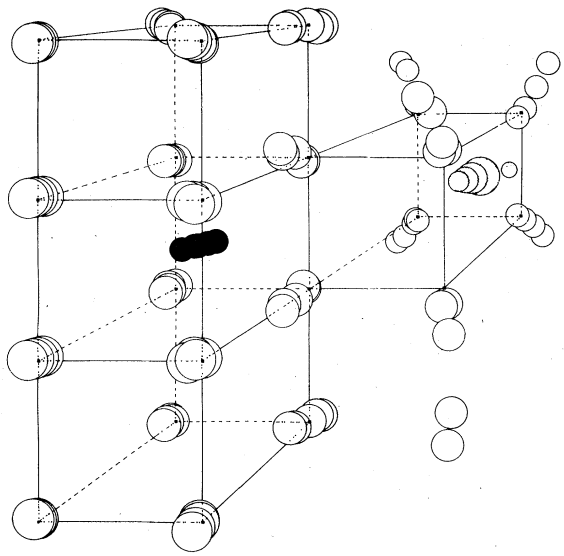

FIG. 8. Schematic three-dimensional representation of some of the ionic positions in region I, resulting from calculations of type B (see also Table IV). For proper comparison with Fig. 4 the corresponding part of region I has been depicted here. Displacements from the lattice sites have been enlarged by a factor of 3.

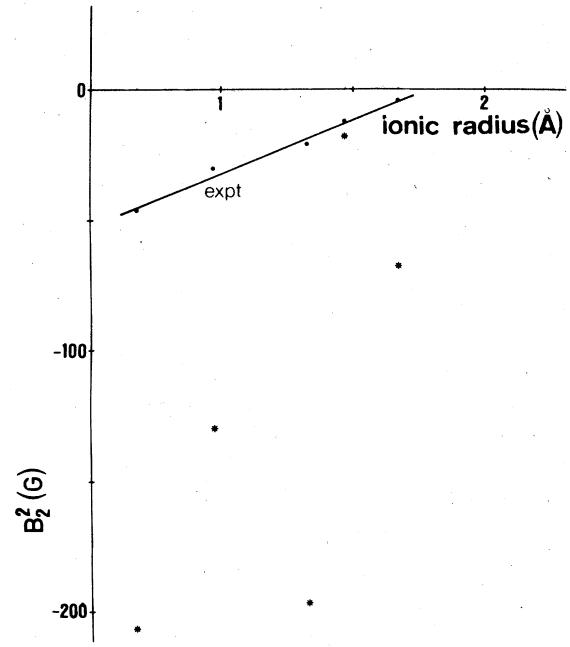

FIG. 10. Calculated and experimental values of B_2^2 as a function of the radius of the M^+ ion.

an interionic distance which is smaller than the sum of the hard core radii of the ions the repulsive energy becomes very large.

Analogous to the treatment given for the calculations of type A we have presented a review of the results in Figs. 8, 9, 10, and 11 and Tables IV and V. In the figures, showing the behavior of B_2^0, B_2^2, and c_1^0 we have included the experimental values. An interesting additional result of the defect calculations is the relative substitution energy of the various monovalent metal ions in the charge compensation complex. The results have been plotted in Fig. 12;

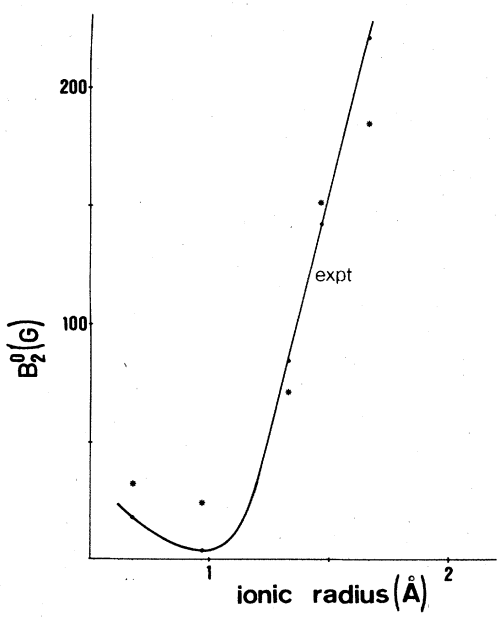

FIG. 9. Calculated and experimental values of the magnetic crystal-field parameter B_2^0, given in Tables III and V, as a function of the radius of the M^+ ion.

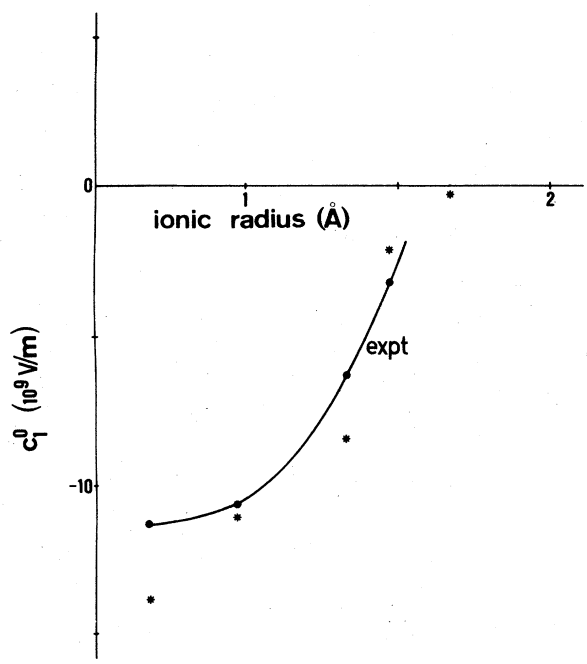

FIG. 11. Calculated and experimental values of c_1^0 as a function of the radius of the M^+ ion.

TABLE IV. Calculated displacements in Å with respect to pure CaF_2 for the ions in region I according to calculation *B*. The numbers in this table, which indicate the ions in region I correspond with the numbers in Fig. 2; the system of axes has been given in Fig. 2. Displacements of ions occupying symmetrical positions with respect to the complex can be deduced from the displacements by symmetry operations.

		Li^+	Na^+	K^+	Rb^+	Cs^+
ion 1:	Δx	0	0	0	0	0
	Δy	−0.096	−0.070	−0.039	−0.029	0.012
	Δz	0.096	0.070	0.039	0.029	−0.012
ion 2:	Δx	−0.013	−0.016	0.053	0.047	0.080
	Δy	0.014	0.019	0.084	0.043	0.092
	Δz	−0.014	−0.019	−0.084	−0.043	−0.092
ion 4:	Δx	−0.019	−0.018	−0.018	−0.013	−0.007
	Δy	−0.002	−0.001	0.022	−0.001	0.017
	Δz	0.002	−0.009	−0.023	−0.051	−0.070
ion 8:	Δx	0.023	0.020	0.021	0.017	0.021
	Δy	−0.014	−0.001	0.005	0.012	0.031
	Δz	0.014	0.001	−0.005	−0.012	−0.031
ion 10:	Δx	0	0	0	0	0
	Δy	−0.496	−0.095	−0.112	−0.130	−0.157
	Δz	0.496	0.095	0.112	0.130	0.157
ion 11:	Δx	−0.033	0.046	0.268	0.512	0.512
	Δy	0.028	−0.014	−0.214	−0.335	−0.335
	Δz	−0.028	0.014	0.214	0.335	0.335
ion 15:	Δx	0.067	0.067	0.166	0.436	0.538
	Δy	0.043	0.069	0.160	0.454	0.577
	Δz	0.045	0.030	0.135	0.344	0.382
ion 17:	Δx	−0.009	−0.013	0.004	0.002	−0.007
	Δy	−0.038	−0.026	0.004	0.053	0.069
	Δz	0.038	0.026	−0.004	−0.053	−0.069
ion 19:	Δx	−0.014	−0.016	−0.011	−0.001	0.010
	Δy	0.007	0.011	0.022	0.048	0.064
	Δz	−0.015	−0.012	−0.002	−0.010	−0.015
ion 23:	Δx	−0.012	−0.016	−0.016	−0.020	−0.019
	Δy	0.019	0.017	0.008	0.007	0.006
	Δz	−0.019	−0.017	−0.008	−0.007	−0.006
ion 25:	Δx	0.037	0.033	0.058	0.126	0.196
	Δy	−0.014	−0.003	0.029	0.083	0.138
	Δz	0.014	−0.010	−0.040	−0.060	−0.112
ion 29:	Δx	−0.015	0.032	0.089	0.194	0.194
	Δy	−0.001	0.020	0.042	0.059	0.057
	Δz	0.001	−0.020	−0.042	−0.059	−0.057
ion 31:	Δx	−0.002	0.001	0.008	0.009	−0.017
	Δy	0.024	0.029	0.049	0.096	0.134
	Δz	−0.035	−0.044	−0.064	−0.133	−0.198
ion 35:	Δx	0.001	0.002	0.011	0.022	0.016
	Δy	−0.010	−0.007	−0.004	0.009	0.007
	Δz	0.011	0.001	−0.017	−0.032	−0.053
ion 39:	Δx	0	0	0	0	0
	Δy	0.034	0.044	0.052	0.054	0.062
	Δz	−0.034	−0.044	−0.052	−0.054	−0.062
ion 40:	Δx	0	0	0	0	0
	Δy	−0.025	0.040	−0.058	−0.111	−0.120
	Δz	0.025	−0.040	0.058	0.111	0.120
ion 41:	Δx	−0.011	0.016	0.079	0.138	0.157
	Δy	−0.089	−0.061	0.001	0.054	0.095
	Δz	0.106	0.108	0.084	0.035	0.000

TABLE V. Calculated values of the crystal-field parameters B_2^0, B_2^2, and c_1^0, obtained from the results of calculation B and formulas (3) and (4) (given in the preceding paper).

	B_2^0 (G)	B_2^2 (G)	c_1^0 (10^9 V/m)
Li^+	30.2	−206.8	−13.9
Na^+	24.6	−129.9	−11.0
K^+	70.1	−196.0	−8.4
Rb^+	151.1	−17.4	−2.1
Cs^+	184.3	−67.2	−0.3

the difference between the values for Li^+ and Cs^+ is about 1.6 eV. (We note that the values for Rb and Cs are not as accurate as those associated with Li^+, Na^+, and K^+ because of the very large displacements of the ions 11–16). From the calculations of type A we find a difference of 3.5 eV. Figure 12 shows that it is easier to introduce Gd^{3+}-Li^+ complexes in CaF_2 than Gd^{3+}-Cs^+, in agreement with our experimental observations. It was found to be quite difficult to introduce sufficient Gd^{2+}-Cs^+ complexes in CaF_2 crystals to carry out EPR experiments.

IV. DISCUSSION

In this paper we have presented an attempt to calculate from the known bulk parameters of CaF_2 and the properties of Gd^{3+} and M^+ (Li^+, . . . , Cs^+) ions the crystal-field splittings associated with first and second degree potentials. Using some selected physical properties of CaF_2 as a basis one is able to calculated the polarizabilities of the ions of the host crystal; in addition the repulsive interactions have been obtained.[1] In this treatment (polarizable-point-charge model) the ions are considered to carry charges of integer values. *We emphasize that in this method we did not employ any fitting procedure to improve the agreement between theory and experiment.*

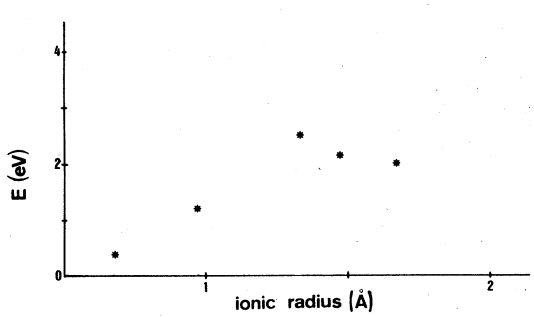

FIG. 12. Total energy of the crystal after the minimization procedure as a function of the M^+ ionic radius. Absolute values of the energies could not be given in this figure because constant terms in the energy expressions have been neglected; the condition of zero energy has been chosen arbitrarily.

From the calculated positions of the ions surrounding the defect we have calculated the important crystal-field parameters c_1^0, B_2^0, and B_2^2 in accordance with the procedures reviewed in Appendix A of the preceding paper. We note that for the description of the even magnetic splitting parameters B_2^0 and B_2^2 we have used Eqs. (3) and (4) given in the previous article. These formulas have not been fitted to describe the experimental results; they have been derived theoretically in Refs. 16 and 17.

An important limitation of our calculations presented in this paper is the restricted number of ions which have been taken into account in the minimization procedure. In order to find the minimum energy of one particular complex in CaF_2 we need of the order of 1 h computing time of the Cyber 74-16 CDC computer. The effect of this limitation is visualized by comparing Figs. 4 and 8, showing that especially the immediate surroundings of the M^+ impurity is affected by the boundary between regions I and II.

In the case of a small region I (24 ions) some of the surrounding ions show rapid variations of minimum energy positions as as a function of the M^+ radius. In particular, the ions referred to as 10–16 behave in a rather irregular way (see Figs. 2 and 4). Considering the behavior of the same ions in the treatment of type B we observe (see Fig. 8) that these ions move gradually as a function of the M^+ radius. From this observation we conclude that the results associated with treatment B are more reliable than those of type A.

It is of interest to compare the theoretically calculated shifts of some of the surrounding ions with the experimental ones as obtained from our electron-nuclear double resonance (ENDOR) work discussed in the previous paper. For a quick review of the results obtained so far we have compiled some of the calculated shifts together with the experimentally observed ones in Table VI. It is immediately clear that there is good agreement between the "ENDOR shifts" and those calculated by means of method B. Except for the theoretical shifts of ions 13–16, method A also gives good results. From Table VI we find support for the conclusion given above that treatment B gives more reliable results than treatment A.

We shall now discuss the results obtained for the crystal-field parameters B_2^0, B_2^2, and c_1^0. From Figs. 5 and 9 it is clear that the theoretical description of B_2^0 is good; especially the trend of this splitting parameter shows good agreement with experiment. From a comparison of the theoretical B_2^0 curves obtained with methods A and B, with the experimentally observed one we conclude that the description by

TABLE VI. Shifts obtained from ENDOR experiments (see Ref. 9) for some ions around a Gd^{3+}-K^+ complex in CaF_2. These shifts are compared to the results of calculations *A* and *B* (see Tables II and IV). The numbers, indicating the ions, correspond with the numbers in Fig. 2.

	Displacement (Å)		
	ENDOR	Calculation *A*	Calculation *B*
ion 1	0.03	0.03	0.06
ion 16	0.28	0.80	0.27
ion 19	<0.05	0.05	0.02
ion 21	0.04	0.05	0.02

method *B* is preferable. A similar conclusion is drawn from a comparison of the theoretical and experimental c_1^0 curves (Figs. 7 and 11).

Significant deviations between theory and experiment are found for the parameter B_2^2. We note, however, that the description of this parameter within methods *A* and *B* is uncertain, probably because region I is too small. An important result is that as a function of the size of M^+ and of region I, large variations of the parameter B_2^2 are found. From the good agreement between theory and experiment for the parameters B_2^0 and c_1^0 and the theoretical and ENDOR displacements we expect that with an increased volume of region I, one should be able to describe the B_2^2 parameter equally well.

Although appreciable efforts have been made to understand and predict the magnetic crystal-field parameters of Gd^{3+} in many solid materials, no clear cut theoretical explanation has been given until now. In this regard we mention the systematic review of the magnetic properties of Gd^{3+} impurities in crystalline hosts by Buckmaster and Shing[18] and the considerable amount of theoretical work done by Newman and Urban[19] and Edgar and Newman.[20] The present study shows that with an extensive theoretical approach we are able to describe the important features of the magnetic splitting parameters of Gd^{3+} in a series of complexes in a strongly ionic material such as CaF_2.

ACKNOWLEDGMENTS

The authors wish to thank Dr. F. Hess for discussions concerning the minimization procedures. This work is part of the research program of the Stichting voor Fundamenteel Onderzoek der Materie and has been made possible by financial support from the Nederlandse Organisatie voor Zuiver Wetenschappelijk Onderzoek.

[1]A. D. Franklin, J. Phys. Chem. Solids 29, 823 (1968).
[2]M. J. Norgett, J. Phys. C 4, 298 (1971).
[3]B. G. Dick and A. W. Overhauser, Phys. Rev. 112, 90 (1958).
[4]M. P. Verma and R. K. Singh, Phys. Status Solidi 33, 769 (1969).
[5]H. Witte and E. Wölfel, Rev. Mod. Phys. 30, 51 (1958).
[6]W. Hayes, *Crystals with the Fluorite Structure* (Clarendon, Oxford, 1974).
[7]J. A. van Winsum, H. W. den Hartog, and T. Lee, Phys. Rev. B 18, 178 (1978).
[8]J. A. van Winsum, T. Lee, H. W. den Hartog, and A. J. Dekker, J. Phys. Chem. Solids 39, 1217 (1978).
[9]E. J. Bijvank and H. W. den Hartog, Phys. Rev. B 22, 4121 (1980) (preceding paper).
[10]C. R. A. Catlow and M. J. Norgett, J. Phys. C 6, 1325 (1973).
[11]C. J. F. Böttcher, *Theory of Electric Polarization* (Elsevier, Amsterdam, 1973).
[12]C. R. A. Catlow, W. Hayes, and M. C. K. Wiltshire, J. Phys. C 10, L243 (1977).
[13]I. M. Boswarva and A. B. Lidiard, Philos. Mag. 16, 805 (1967).
[14]F. Hess (private communication).
[15]A. Abragam and B. Bleaney, *Electron Paramagnetic Resonance of Transition Ions* (Clarendon, Oxford, 1970).
[16]E. J. Bijvank, H. W. den Hartog, and J. Andriessen, Phys. Rev. B 16, 1008 (1977).
[17]A. N. Lefferts, E. J. Bijvank, and H. W. den Hartog, Phys. Rev. B 17, 4214 (1978).
[18]H. A. Buckmaster and Y. H. Shing, Phys. Status Solidi (a) 12, 325 (1972).
[19]D. J. Newman and W. Urban, Adv. Phys. 24, 793 (1975).
[20]A. Edgar and D. J. Newman, J. Phys. C 8, 4023 (1975).